

Spin-lattice relaxation in Si quantum dots

B. A. Glavin^{1,2} and K. W. Kim²¹*Institute of Semiconductor Physics, Ukrainian National Academy of Sciences, Pr. Nauki 45, Kiev 03028, Ukraine*²*Department of Electrical and Computer Engineering, North Carolina State University, Raleigh, North Carolina 27695-7911, USA*

(Received 25 November 2002; revised manuscript received 24 March 2003; published 17 July 2003)

We consider spin-lattice relaxation processes for electrons trapped in lateral Si quantum dots in a [001] inversion layer. Such dots are characterized by strong confinement in the direction perpendicular to the surface and much weaker confinement in the lateral direction. The spin relaxation is assumed to be due to the modulation of electron g -factor by the phonon-induced strain, as was shown previously for the shallow donors. The results clearly indicate that the specific valley structure of the ground electron state in Si quantum dots causes strong anisotropy for both the one-phonon and two-phonon spin-relaxation rates. In addition, it gives rise to a partial suppression of the two-phonon relaxation in comparison to the spin relaxation of donor electrons.

DOI: 10.1103/PhysRevB.68.045308

PACS number(s): 68.65.Hb, 76.30.-v

I. INTRODUCTION

Recently, there is growing interest in the physics of electron spin due to the enormous potential of spin-based devices. In these so-called “spintronic” devices, information is encoded in the spin state of individual electrons. Numerous concepts ranging from spin analogs of conventional electronic devices, to quantum computers (which utilize the Zeeman doublet of a confined electron as a qubit)¹ have been proposed. Electron-spin states relax by scattering with imperfections or elementary excitations such as phonons. Hence, the spin-relaxation time is a vital characteristic that determines the potential value of a spin-based device.

In particular, considerable attention has been devoted to the spin properties of electrons confined in artificial semiconductor quantum dots (QD's). For QD based on III-V compounds, spin relaxation is mainly caused by the so-called admixture mechanism,² which originates from the lack of spatial inversion symmetry in these materials. As a result, the electron states in a magnetic field are not pure in spin. This, in turn, gives rise to the finite coupling of the Zeeman-doublet states by the phonon deformation or piezoelectric potentials. In addition to the spin-lattice relaxation, spin decoherence can be due to the fluctuating magnetic field caused by the nuclear spins and the spins of the electrons confined in the neighboring QD's.³ As with the spin-lattice relaxation, this effect also provides an important parameter in estimating the validity of device concepts.

In the present paper, we calculate the longitudinal spin-lattice relaxation time T_1 for electrons confined in Si QD's. Being a relatively light semiconductor, Si is characterized by a weak spin-orbit interaction, which basically determines the strength of spin relaxation. In addition, only a small fraction of the isotopes in natural Si possess a nonzero nuclear magnetic moment. As a result, the electron-nuclear spin-flip process is expected to be slow. These two properties of Si, along with the tempting possibility of integrating the “quantum” part of a computer with the well-developed Si “classical” electronics, make Si an attractive material for spin devices.

We concentrate on particular design of a QD based on a [001] inversion layer formed at the interface of Si and SiO₂

[see Fig. 1(a)]. The lateral confinement of electrons is assumed to be due to the attractive potential applied to the gate electrode deposited on top of the oxide layer. In our calculations, we take advantage of the results obtained for spin relaxation of shallow-donor electrons in Si.^{4–8} In Refs. 6–8, the spin-lattice relaxation was assumed to be due to the modulation of electron g factor by the phonon-induced strain. The parameters of the effective Hamiltonian were estimated from microscopic models. Later, they were also determined by measuring the g factor under a static strain.⁴ We

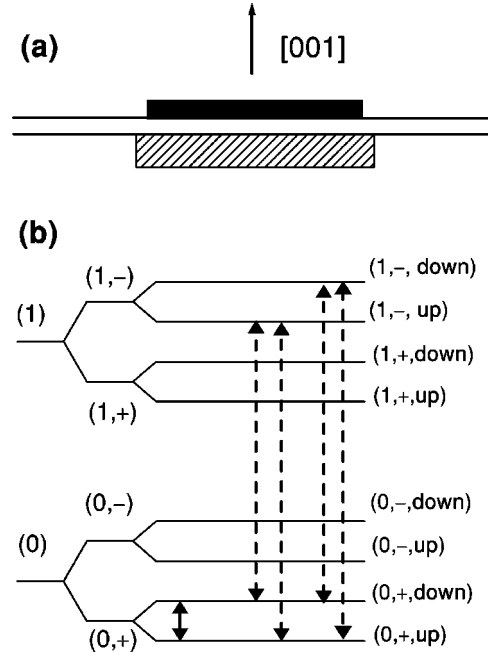


FIG. 1. (a) Schematics of the lateral QD. Confinement in the [001] direction is achieved as in the conventional inversion layers, while the lateral confinement is provided by the electrodes (black boxes). (b) Schematic illustration of energy levels in lateral QD's. (0) and (1) mark the different states of lateral confinement. Valley-split + and - states are further split by the magnetic field into spin-up and spin-down states. The solid (dashed) arrows show electron transitions under one-phonon (two-phonon) relaxation.

conclude that the specific valley structure of the electron states in lateral QD's modifies essentially both the single-phonon and two-phonon relaxation. In particular, we predict that for the [001] inversion layer, the spin relaxation is suppressed if the applied magnetic field is parallel to the [001] or [110] direction. In addition, it is found that the two-phonon relaxation in lateral QD is much weaker than for shallow donors. Simple analytical expressions are obtained for the two limiting cases, namely, for $T \ll E_Z$ and $T \gg E_Z$, where T is the temperature in energy units and E_Z is the Zeeman-doublet splitting energy. The former case is more relevant to the conditions for quantum computation, while the latter is close to the typical conditions of electron paramagnetic resonance measurements. For the resonance frequency of about 50 GHz, and a low enough temperature, the spin-relaxation time is found to be several minutes with the single-phonon process providing the prevailing contribution to relaxation. For elevated temperatures, the two-phonon process becomes significant and the relaxation time can be substantially smaller.

An alternative QD design based on Si/SiGe heterostructures is also possible. However, the SiGe-based design may face additional complications for quantum computing applications. For example, electron confinement in Si/SiGe heterostructures is relatively weak and the penetration of electron wave function to the SiGe barriers is inevitable. Since spin-orbit interaction in Ge is stronger than in Si, these structures are expected to have higher spin-relaxation rates. One more important feature of Si/SiGe quantum wells is considerable strain caused by mismatch of Si and SiGe lattices. The influence of these effects on spin relaxation for donors and lateral QD's has been analyzed recently in Ref. 9. However, it⁹ considers only one of the two main contributions to the g -factor modulation. One consequence of this simplification is that its prediction for the relaxation rate at high strain is too optimistic.

The rest of the paper is organized as follows: In Sec. II, we introduce the Hamiltonian for spin-lattice relaxation and provide expressions for the single-phonon and the two-phonon relaxation rates. In Sec. III, the asymptotic dependences for different temperatures as well as numerical results are presented. Finally, Sec. IV is devoted to the discussion of the obtained results along with other potential mechanisms of spin-lattice relaxation.

II. EFFECTIVE HAMILTONIAN FOR SPIN-LATTICE RELAXATION

For crystals which possess inversion symmetry like Si, there is no analog of conventional deformation potential for the spin-flip process, which is often called Van Vleck cancellation.¹⁰ This is a direct result of the requirement for the Hamiltonian to be invariant under a generalized inversion transformation $C=JK$, where J and K are spatial and time inversion operators. In Refs. 6–8, the following effective C -invariant Hamiltonian describing the modulation of electron g factor by strain has been proposed:

$$H_g = A_{ijkl} u_{ij} B_k \sigma_l, \quad (1)$$

where A_{ijkl} are the coefficients, u_{ij} is the strain tensor, B_k are the components of the magnetic field, and σ_l are the Pauli matrices; here and below we assume summation over the repeated indices. H_g is written in the basis of the Bloch functions corresponding to the bottom of the conduction band and can be used for the calculation of spin transitions for any electron state described within the effective-mass approximation. Hence, the formalism developed originally for the spin-relaxation properties of shallow donor electrons can be applied to the case of electrons confined in artificial QD's. Nonzero coefficients A are determined by the symmetry of the crystal using the method of invariants.¹¹ For III-V materials, such a Hamiltonian was used for the spin-lattice relaxation analysis in Ref. 2. For the Δ point of the Brillouin band in a diamondlike crystal which corresponds to the conduction band of Si, there are eight invariants and the Hamiltonian for a [001] valley can be written as¹²

$$\begin{aligned} H_g^{[001]} = & \frac{1}{2} \mu_B [A_1 \sigma_z B_z (u_{xx} + u_{yy}) + A_2 \sigma_z B_z u_{zz} \\ & + A_3 \sigma_z (B_x u_{xz} + B_y u_{yz}) + A_4 (\sigma_x B_x + \sigma_y B_y) u_{zz} \\ & + A_5 (\sigma_x B_x + \sigma_y B_y) (u_{xx} + u_{yy}) \\ & + A_6 (\sigma_x B_y + \sigma_y B_x) u_{xy} + A_7 (\sigma_x u_{xz} + \sigma_y u_{yz}) B_z \\ & + A_8 (\sigma_x B_x - \sigma_y B_y) (u_{xx} - u_{yy})]. \end{aligned} \quad (2)$$

Here we introduced the factor $\mu_B/2$ for convenience, μ_B being the Bohr magneton. The absolute values of the coefficients A can be determined, in principle, by using a many-band effective-mass expansion of the electron wave function in a uniform magnetic field, similar to that used in Ref. 7. In practice, this cannot be accomplished since the required momentum matrix elements are unknown. However, some qualitative considerations are possible. Since the terms of the expression for g factor contain the energy gaps between the coupled bands in the denominator, coupling of the closest bands is expected to be the strongest. For Si, there is a Δ'_2 band which is close to the Δ_1 conduction band. These bands merge at the X point in the momentum space but are not coupled by either a spin-orbit interaction or momentum operators. Therefore, $\Delta_1 \leftrightarrow \Delta'_2$ coupling is not manifested in the effective mass or g factor of unstrained Si. However, these bands are coupled by the deformation potential. From the character tables of the Δ point and the corresponding invariants, it is easy to conclude that this coupling is realized by the deformation potential term proportional to u_{xy} . Since H_g contains only one invariant proportional to u_{xy} , it can be concluded that the major contribution to the Hamiltonian is

$$H_g^{[001]} = \frac{1}{2} A \mu_B (\sigma_x B_y + \sigma_y B_x) u_{xy}, \quad (3)$$

where we drop the index of the coefficient A_6 . This argument was initially used by Roth.⁸

To proceed with the calculation of the longitudinal relaxation time T_1 , we need to describe explicitly the system under consideration as well as the characteristic energy and length scales. As mentioned in the Introduction, we consider Si lateral QD's formed at the Si/SiO₂ interface, where the lateral confinement is due to the gate electrodes. For such a

system, the lateral dimension of the QD a_{lat} is typically on the order of one hundred nanometers, exceeding considerably the inversion layer thickness a_{2D} . The energy structure of the electron levels is determined by the following parameters: (a) quantization energy in the two-dimensional (2D) inversion channel $E_{2D} \sim \hbar^2 / (2m_{2D}a_{2D}^2)$; (b) lateral quantization energy $E_{lat} \sim \hbar^2 / (2m_{lat}a_{lat}^2)$; (c) intervalley-splitting energy between $[001]$ and $[00\bar{1}]$ states, Δ ; and (d) Zeeman energy $E_Z = \mu_B g B$, where g is the effective g factor of the confined electrons depending, in general, on the direction of the magnetic field. Here, m_{2D} and m_{lat} are the electron effective masses in the direction normal and parallel to the inversion layer, respectively. For the $[001]$ inversion layer, they just correspond to the longitudinal and transverse effective masses of Si. In the following, we assume that the conditions $E_Z \ll \Delta$, E_{lat} are satisfied. This allows a perturbative treatment of the Zeeman term in the Hamiltonian. In fact, this is also a necessary requirement for spin qubit operation. Using modern technology, E_{lat} can be made about 1 meV, which corresponds to a_{lat} in the range of several tens of nanometers. In contrast, Δ can be controlled in a much lesser degree. For $a_{lat} \gg a_{2D}$, which is a typical condition, the valley splitting in a lateral QD is the same as in the corresponding quantum well which is roughly proportional to the confining electric field in an inversion layer. Experimentally, Δ was measured to be up to 1 meV in strong fields (see Ref. 13). In Fig. 1(b), we show schematically the energy levels and the electron transitions under consideration. The numbers “0” and “1” mark the levels of lateral electron confinement. The signs + and - denote the valley-split electron states, and “up” and “down” are the spin states. We assume that only the lowest Zeeman doublet can be populated, which means that the temperature T is much less than Δ and E_{lat} . The longitudinal relaxation time T_1 is determined as $T_1^{-1} = W_{up-down} + W_{down-up}$, where W are the probabilities of spin-up to spin-down and spin-down to spin-up transitions. The solid arrows indicate the single-phonon transitions, while the dashed arrows correspond to the two-phonon process. Later in this section, we comment on the possible two-phonon processes shown in the figure.

In Refs. 6 and 7, an alternative Hamiltonian to Eq. (3) was considered. It originates from the coupling of the donor singlet and doublet states by an applied magnetic field. It arises due to the different valley structure of these states and the anisotropy of the g factor in the individual valleys. Although this Hamiltonian does not involve $\Delta \leftrightarrow \Delta'_2$ coupling, its contribution is high because of a very small gap between the singlet and doublet states. However, there is no such mechanism in the $[001]$ lateral QD's, which is probably the main difference with the case of spin relaxation for donor electrons. The reason for that can be easily seen. For the $[001]$ inversion layer, the ground electron state is a combination of $[001]$ and $[00\bar{1}]$ states:

$$\Psi_{\pm} = \chi(F_{001}^{\pm} \psi_{001} + F_{00\bar{1}}^{\pm} \psi_{00\bar{1}}), \quad (4)$$

where we dropped the spin index of wave functions. Here χ is the envelope wave function, ψ_{001} and $\psi_{00\bar{1}}$ are the Bloch

functions corresponding to the $[001]$ and $[00\bar{1}]$ valleys, respectively, and F are the coefficients which determine the valley splitting. Particular expressions for F can be found using a microscopic model, for example, that of Sham and Nakayama.¹⁴ In our case, we do not need explicit expressions for C . It is enough to use the fact that Zeeman Hamiltonian has identical forms for the $[001]$ and $[00\bar{1}]$ valleys and its intervalley matrix elements are zero. Therefore, the matrix element between Ψ_+ and Ψ_- , which is proportional to the overlap between them, is zero because these states are orthogonal.

The Hamiltonian of Eq. (3) is written in the representation where the basis electron wave functions correspond to the definite spin projections on the z axis. For calculation of T_1 , it must be rewritten by using a representation with the definite spin projection on the direction of the magnetic field.¹⁵ This can be done following the standard procedure of transformation for spin operators rotation.¹⁶ Finally, we obtain the expression for the one-phonon relaxation rate $1/T_1^{(1)}$ as

$$\begin{aligned} \frac{1}{T_1^{(1)}} &= \frac{\pi^3 A^2}{4} \frac{\hbar f^5}{g^2 \rho} (1 + 2N_T) \\ &\times \sin^2 \theta (\cos^2 2\phi + \cos^2 \theta \sin^2 2\phi) \\ &\times \sum_i \int d\Omega_q^{(i)} \frac{(e_x^{(i)} n_y^{(i)} + e_y^{(i)} n_x^{(i)})^2}{s_i^5}. \end{aligned} \quad (5)$$

In this equation, g is the slightly anisotropic g factor of confined electrons, $f = g \mu_B B / (2 \pi \hbar)$ is the resonance frequency, θ and ϕ are the spherical angles of the magnetic field, ρ is the material density, N_T is the Planck phonon population for the energies equal to E_Z , Ω_q is a solid angle in the phonon wave-vector space \mathbf{q} , \mathbf{e} , and \mathbf{n} are the phonon polarization vector and the unit vector parallel to \mathbf{q} , respectively, s is the sound velocity, and the summation is over the acoustic-phonon branches. Equation (5) assumes that the phonon wavelength corresponding to the energy E_Z is much greater than the lateral dimensions of QD. In this case, the form factor of the electron-phonon interaction is equal to unity and $T_1^{(1)}$ does not depend on the particular shape of the lateral confining potential. To check the validity of this approach, we performed calculations of $T_1^{(1)}$ assuming parabolic lateral confinement and found that for the lateral level separation of 1 meV, the obtained correction is less than 10% even for $f = 50$ GHz. That is not surprising since for the parameter under consideration, the characteristic wavelength of the transverse acoustic phonons is a few times larger than a_{lat} . An additional assumption of the bulklike phonon spectrum is made for simplicity. This probably introduces a greater error since the lateral QD's are normally situated close to the surface. As shown in Refs. 17–19, the phonon modes in this case are essentially rebuilt, due to the interference of the incident and reflected phonons as well as the origination of Rayleigh waves, which strongly modify electron-phonon coupling.

Equation (5) predicts strong anisotropy of the relaxation rate. If the magnetic field is parallel to the $[001]$ or $[110]$

direction, $T_1^{(1)}$ goes to infinity. When rewritten for the basis with the definite spin projection on the direction of the magnetic field, the Hamiltonian of Eq. (3) vanishes for these particular orientations. Of course, in experiments the relaxation for these cases is not expected to be suppressed completely, since the remaining terms of Eq. (2) also give rise to spin flip. However, their contribution to the relaxation rate is expected to be much smaller, with a factor of about $[(E_{\Delta_2'} - E_{\Delta_1})/(E_{\Delta_1} - E_{\Delta_3})]^2 \sim 5 \times 10^{-2}$, where E_{Δ} is the energy of the corresponding electron branch at the Δ point of the momentum space. Therefore, a significant decrease of the relaxation rate is expected for the magnetic-field directions indicated above. It is also worth mentioning that the Hamiltonian similar to Eq. (3) does not provide such strong anisotropy in the case of shallow donors (see Ref. 4). This is due to the fact that the ground state of a donor electron in Si is a uniformly weighted combination of all six valleys. Consequently, the relaxation rate is determined by the sum of the partial contributions of each valley. For a magnetic field parallel to the [001] or [110] direction, only the matrix element for the [001] and [00 $\bar{1}$] valleys vanishes and that for the remaining four valleys does not. As a result, the cumulative matrix element does not go to zero for any direction of magnetic field.

Assuming an isotropic acoustic-phonon spectrum, we obtain

$$\frac{1}{T_1^{(1)}} = \frac{2\pi^4 A^2}{5} \frac{\hbar f^5}{g^2 \rho_s^5} (1 + 2N_T) \times \sin^2 \theta (\cos^2 2\phi + \cos^2 \theta \sin^2 2\phi). \quad (6)$$

Here, we take into account only transverse acoustic phonons, which provide the major contribution to the relaxation rate.

Let us now turn to the calculation of the relaxation time due to the two-phonon transitions $T_1^{(2)}$. This is a second-order transition where the electron is virtually scattered first to an intermediate state and then to the final state. One of the virtual transitions is accompanied by spin flip, while the other occurs with spin conservation. The probability of a two-phonon transition can be found using the second-order perturbation theory (see, for example, Ref. 20). For the spin relaxation of donor electrons, the intermediate electron state is represented by the excited doublet. In contrast, for the case of [001] lateral QD, the valley-split state cannot serve as an intermediate state. This is because the valley-split states are not coupled by the Hamiltonian of Eq. (2). This can be shown using an argument similar to that applied for the proof of the absence of g factor modulation due to coupling of the valley-split states. Other possible transitions are through the excited states of the lateral confinement. Since the intervalley splitting is controlled by the electron confinement in the z direction rather than in the lateral direction, these transitions are actually possible between the states having the same valley structure [see Fig. 1(b)]. If the phonon wave vector is very small, then the probability of such a transition goes to zero because the overlap functions of 0 and 1 states are orthogonal. To determine the probability of two-phonon tran-

sition for a finite phonon wave vector, we need to know the overlap function χ explicitly. For calculations, we assume parabolic lateral confinement. In this case, the ‘‘lateral’’ electron state is determined by the two quantum numbers l_x and l_y . The 0 state corresponds to $l_x=0$, $l_y=0$, and there are two degenerate 1 states with $l_x=0$, $l_y=1$ and $l_x=1$, $l_y=0$. Using the expressions for the wave functions of harmonic oscillator,¹⁶ it is easy to obtain the necessary form factor J ,

$$J \equiv \int dx dy dz \chi_{00} \chi_{10} \exp[i(q_x x + q_y y + q_z z)] = \frac{1}{\sqrt{2}} \frac{q_x}{k} \exp\left(-\frac{q_x^2 + q_y^2}{4k^2}\right), \quad (7)$$

where the subscript of χ represent the l_x and l_y quantum numbers and k is expressed through the energy gap δ between 0 and 1 states and the lateral effective mass: $k = \sqrt{m_{lat} \delta / \hbar}$. Here, we take into account that the thickness of the inversion layer is much less than the typical phonon wavelength. In the following, we also assume that the typical phonon wave-vector is less than k , and drop the exponent in the expression for J . Note that J can be modified due to the diamagnetic influence of the magnetic field as well. In particular, it can lift the degeneracy of 1 states. In our calculations, we do not consider this effect.

We can distinguish three contributions to the two-phonon relaxation rate: (a) due to emission of two phonons, (b) due to absorption of two phonons, and (c) due to phonon scattering. For each of them the rate can be expressed in a uniform manner:

$$\frac{1}{T_1^{(2)}} = 34\pi^{10} \left(\frac{16}{105}\right)^2 \frac{A^2 E_2^2 \hbar^6 f^{13}}{\delta^4 g^2 \rho^2 s_i^{14} m_{lat}^2} \times \sin^2 \theta (\cos^2 2\phi + \cos^2 \theta \sin^2 2\phi) D_i. \quad (8)$$

Here, only the transverse phonons are taken into account, which provide the major contribution to the relaxation rate. We also assume that typical phonon energies are considerably less than δ . The spin-conserving virtual transition is treated within the deformation model, which for the [001] valley provides the interaction $E = E_1 u_{ii} + E_2 u_{zz}$, where E_1 and E_2 are the deformation potential constants. The coefficients D depend on temperature and they are different for each of the three processes mentioned:

$$D_{em} = \int_0^1 dx x^5 (1-x)^5 \left(1 + \frac{1}{\exp(x/t) - 1}\right) \times \left(1 + \frac{1}{\exp[(1-x)/t] - 1}\right), \quad (9)$$

$$D_{ab} = \int_0^1 dx x^5 (1-x)^5 \frac{1}{\exp(x/t) - 1} \frac{1}{\exp[(1-x)/t] - 1},$$

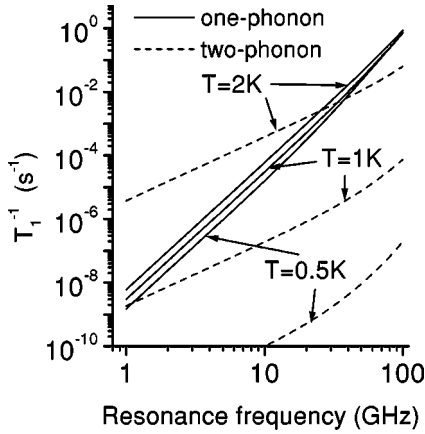


FIG. 2. Dependence of the one-phonon (solid lines) and two-phonon (dashed lines) spin-relaxation rates on resonance frequency for temperatures of 0.5 K, 1 K, and 2 K.

$$D_{scat} = \frac{20}{17} \left[\int_0^\infty dx x^5 (1+x)^5 \frac{1}{\exp(x/t) - 1} \right. \\ \times \left(1 + \frac{1}{\exp[(1+x)/t] - 1} \right) + \int_0^\infty dx x^5 (x+1)^5 \\ \times \left. \frac{1}{\exp[(x+1)/t] - 1} \left(1 + \frac{1}{\exp(x/t) - 1} \right) \right],$$

where $t = T/E_Z$. One can see that the two-phonon relaxation rate is characterized by the same anisotropy as in the one-phonon relaxation rate. In the following section, we analyze the asymptotic dependences of the relaxation rates for different temperature regimes and perform numerical calculations.

III. RELAXATION RATES FOR LOW AND HIGH TEMPERATURES: NUMERICAL RESULTS

For the limiting cases of $T \ll E_Z$ and $T \gg E_Z$, the relaxation rates obey simple power laws as a function of resonance frequency and temperature. In particular, $T_1^{(1)} \sim f^{-5}$ in the former case and $T_1^{(1)} \sim f^{-4} T^{-1}$ in the latter case. This is similar to the case of donor spin relaxation.⁶⁻⁸ The two-phonon relaxation time for $T \ll E_Z$ is proportional to f^{-13} with the main contribution from the two-phonon emission. For $T \gg E_Z$, the relaxation is mainly due to the phonon scattering and $T_1^{(2)} \sim f^{-2} T^{-11}$. For donor electrons, Roth obtained a different power law.⁷ This is because for donor electrons the form factor of singlet-doublet transition in the lowest approximation is equal to unity, in contrast to Eq. (7) for the lateral QD where the form factor is suppressed for long-wavelength phonons.

In Figs. 2 and 3, we show the results of numerical calculations for the one-phonon and two-phonon rates. We assume a magnetic field parallel to the [100] direction, $\rho = 2329 \text{ kg/m}^3$, the transverse sound velocity $s_t = 5420 \text{ m/s}$, $E_Z = 10 \text{ eV}$, $m_{lat} = 0.19m_0$, $\delta = 2 \text{ meV}$, and $g = 2$. The coefficient A can be determined by the measurement of the donor g factor in strained Si. With this method, $A = 1.32$ was obtained in Ref. 4. The dependence of the spin-relaxation rate

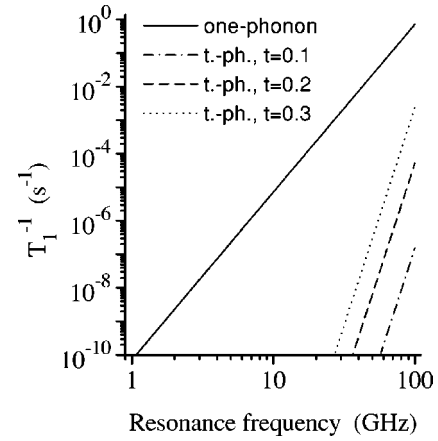


FIG. 3. Dependence of the spin-relaxation rates on resonance frequency for the case where the ratio of temperature and Zeeman splitting t is kept constant. The one-phonon rates for the considered values of this ratio cannot be resolved on this scale and is presented by one curve.

on the resonance frequency is presented in Fig. 2 for several temperatures. One can see that for $T_1^{(1)}$, the transition between the described power dependences at the different temperature regimes is quite fast. This is not the case for $T_1^{(2)}$, which is due to the different temperature dependence of phonon absorption, emission, and scattering rates.

In Fig. 3, we plot the relaxation rates as a function of f under the condition $T/E_Z = \text{const}$. This is relevant to the case of QD-based qubit, where this ratio must be kept small to ensure initial-state preparation of the qubits. We see that under this condition the major contribution is provided by one-phonon scattering.

Of course, the predicted huge relaxation times for small resonance frequencies can be hardly measured in experiments. This is similar to the case of donor spin relaxation,⁴ where actual experiments were undertaken for f about tens of gigahertz.

IV. DISCUSSION

Let us first summarize the major distinction of the spin-relaxation process for lateral QD's and shallow donors. First, we predict that the relaxation for lateral QD's is more anisotropic than that for donor electrons. In particular, for [001] inversion layer the relaxation rate is suppressed for a magnetic field parallel to the [001] or [110] direction. Second, the two-phonon relaxation in lateral QD's is, in general, weaker than for donor electrons and is characterized by different power dependences on the resonance frequency and temperature. Both of these features arise due to the different valley structure of the electron states in lateral QD's in comparison to that of donor electrons. This valley structure in the case of inversion layer-based QD is due to the electron confinement. It is worth mentioning that similar effect can be realized by means of uniaxial strain. This can take place for Si/SiGe heterostructures as well as for donors in intentionally strained crystals.

We have to stress that the first conclusion relies on the

model used for calculations, which must be checked by experiments. This is because the values of the coefficients A_n in Eq. (2) are determined not only by the energy gaps between the bands, but also by a number of interband matrix elements, which are unknown. Strictly speaking, the experiments with donors cannot be considered as a rigorous proof of single-valley Hamiltonian of Eq. (3). In fact, for the donor electrons, eight invariants of Eq. (2) are transformed to three invariants after summation over the valleys. The term measured in Ref. 4, $H \sim u_{xy}(\sigma_x B_y + \sigma_y B_x) + cp$ where cp stands for cyclic permutations, is obtained from several terms of Eq. (2), not only from that of Eq. (3).

There is another mechanism that can modify the spin relaxation in the lateral QD's. This can take place if some quantum levels originated from the longitudinal $[001]$, $[00\bar{1}]$ valleys and the transverse $[100]$, $[\bar{1}00]$, $[010]$, $[0\bar{1}0]$ valleys come close. In this case, the intervalley coupling can mix these two groups. Mixing of these states and the ground

state of the QD by both steady-state and strain-induced contributions of Zeeman Hamiltonian can be possible. As a result, both one-phonon and two-phonon relaxation will be modified. According to self-consistent calculations,¹³ such a situation is possible for particular parameters of Si inversion layer.

Finally, we would like to stress that the electron-spin relaxation in QD's is of the same order of magnitude as that obtained for donors. It is much longer than the T_1 in III-V compounds, which proves a good perspective of Si for quantum information processing.

ACKNOWLEDGMENTS

The work performed at North Carolina State University was supported by the Office of Naval Research and the Defense Advanced Research Projects Agency.

-
- ¹D. Loss and D.P. DiVincenzo, Phys. Rev. A **57**, 120 (1998).
²A.V. Khaetskii and Y.V. Nazarov, Phys. Rev. B **64**, 125316 (2001).
³R. de Sousa and S. Das Sarma, Phys. Rev. B **67**, 033301 (2003).
⁴D.K. Wilson and G. Feher, Phys. Rev. **124**, 1068 (1961).
⁵A. Honig and E. Stupp, Phys. Rev. **117**, 69 (1960).
⁶H. Hasegawa, Phys. Rev. **118**, 1523 (1960).
⁷L. Roth, Phys. Rev. **118**, 1534 (1960).
⁸L. Roth, in *Proceeding of International Conference on Phys. Semiconductions 1960*, edited by K. Mizek (Publishing House of the Czechoslovak Academy of Sciences, Prague, 1961), p. 592.
⁹C. Tahan, M. Friesen, and R. Joynt, Phys. Rev. B **66**, 035314 (2002).
¹⁰J.H. Van Vleck, Phys. Rev. **57**, 426 (1940).
¹¹G. L. Bir and G. E. Pikus, *Symmetry and Strain-Induced Effects in Semiconductors* (Wiley, New York, 1974).
¹²V. I. Sheka (private communication).
¹³T. Ando, A.B. Fowler, and F. Stern, Rev. Mod. Phys. **54**, 437 (1982).
¹⁴L.J. Sham and M. Nakayama, Phys. Rev. B **20**, 734 (1979).
¹⁵It is worth noting that such wave functions are not the eigenfunctions of the Hamiltonian when spin-lattice coupling is not considered. This is a result of the anisotropy in the electron g factor. For Si, this anisotropy is very weak and is not taken into account.
¹⁶L. D. Landau and E. M. Lifshitz, *Quantum Mechanics: Non-relativistic Theory* (Pergamon, Oxford, 1977).
¹⁷S.M. Badalyan and I.B. Levinson, Fiz. Tverd. Tela **30**, 2764 (1988) [Sov. Phys. Solid State **30**, 1592 (1988)].
¹⁸Y.M. Sirenko, K.W. Kim, and M.A. Stroscio, Phys. Rev. B **56**, 15770 (1997).
¹⁹V.I. Pipa, F.T. Vasko, and V.V. Mitin, J. Appl. Phys. **85**, 2754 (1999).
²⁰V. E. Gantmakher and Y. B. Levinson, *Carrier Scattering in Metals and Semiconductors* (North-Holland, Amsterdam, 1987).